17th Australasian Fluid Mechanics Conference
Auckland, New Zealand
5-9 December 2010

Laminar-Turbulent Transition of the Flat-Plate Boundary Layer by a Line of Roughness Elements (Development of Turbulent Quantities within Turbulence Wedges)

M. Ichimiya and Y. Fujiwara

Department of Mechanical Engineering
University of Tokushima, Tokushima, 770-8506 JAPAN

Abstract

Experiments were performed to investigate the effect of a line of roughness elements on flat-plate boundary layer transition. Each of the 11 roughness elements was a cylinder 2 mm in both diameter *d* and height *k*, forming a row in the spanwise direction. Wedge-shaped turbulent regions ("turbulence wedges") developed downstream from the respective roughness elements. Further downstream, two adjacent wedges merged and a two-dimensional turbulent boundary layer was then formed. Mean and fluctuating velocities were measured by hot wire anemometers inside and outside the wedge regions, and intermittency factors were obtained. The process by which the three-dimensional turbulence wedges change into a two-dimensional boundary layer was examined.

The laminar-turbulent transition processes in the downstream direction were examined on two spanwise stations; one is the station on the center line of the roughness element, Z (= z / d) = 0, and the other is the mid-point of the roughness elements, Z = 6(z is the spanwise distance from the center line). At first, the fluctuating velocity overshot Spalart distribution of DNS (R_θ = 300). Next, it decreased and undershot the Spalart distribution, eventually coinciding with it (R_θ = 670). These processes appeared more upstream with Z = 0 than Z = 6. The transition process is induced by the roughness element at Z = 0, whereas it is induced by the interference of two adjacent wedges at Z = 6.

Introduction

The laminar-turbulent transition of boundary layers has been investigated for many years. Among these investigations, artificial transitions due to a roughness element have also been examined [2]. A wedge-shaped turbulent region, or "turbulence wedge" is formed downstream of a single three-dimensional roughness element. The present authors showed in previous studies that just behind the roughness element were many streamwise vortices; on the other hand, further downstream a pair of streamwise vortices was found on both interfaces between the wedge and the outer laminar region [3, 4].

In practice, however, multiple roughnesses are found. Using such multiple roughnesses, Gibbings et al. [1] showed the start and end points of the transition; however, the way in which the structures in the turbulence wedge are affected by an encounter and the interaction between wedges has not been clarified. The present study aims to investigate the transition processes due to a spanwise roughness row, which consists of three-dimensional roughnesses. In particular, this investigation examined turbulent quantities both on a center line of a roughness element and on a mid-point of roughness elements.

Experimental Apparatus and Measurement Methods

The experimental setup consisted of a 15-mm-thick, 400-mm-wide, and 2-m-long Bakelite flat plate with a sharpened leading edge. The plate was mounted horizontally in an open circuit blowing-type wind tunnel. The test section was 400×150 mm^2 in cross section and 2 m in length with a contraction ratio of 10 and a turbulence level of 0.2% at a nominal free stream velocity of 7.5 m/s. Tani et al. [7] showed that the turbulence intensity does not affect the condition of a transition induced from the roughness position. A wall opposite the working side of the plate permitted adjustments of the zero pressure gradient. The velocity profile near the leading edge was of the Blasius type. The experiment was conducted under the condition of the constant unit Reynolds number U_m / ν = 5×10^5 m^{-1}. The reference main flow velocity at the leading edge U_m was about 7.5 m/s.

Figure 1 shows the coordinate system and turbulence wedges. Each roughness element was a cylinder 2 mm in both diameter *d* and height *k*. Eleven elements built up a row in the spanwise direction at 100 mm downstream from the leading edge of the flat plate. The clearance between roughnesses, *s*, was 22 mm, i.e., *s* / *d* equalled 11. A turbulence wedge was formed downstream of the respective roughness. Since the boundary layer at this position without the roughness element was laminar with a thickness of about 2.2 mm, the height of the roughness element *k* was nearly equal to the boundary layer thickness. The roughness Reynolds number based on *k* and velocity at $y = k$ was 996, thus satisfying the condition under which the turbulence wedge develops from the roughness [5, 7]. Here we employ normalized coordinates, X (= (x - x_k) / k), Y (= y / k) and Z (= z / k) (x_k is the x position of the roughness, 100 mm).

A Single hot-wire probe with a tungsten sensing element 5 μm in diameter and 1 mm wide was used in the measurements. The output voltage from the hot wire was digitized at a 10-kHz sampling frequency during an approximately 26-second sampling

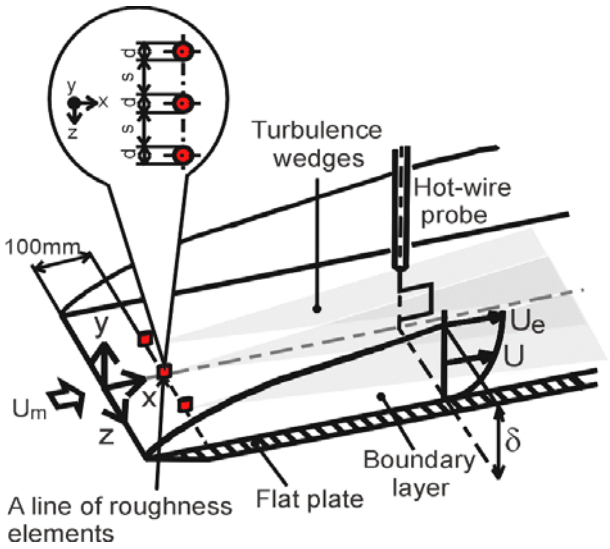

Figure 1. Coordinate system and turbulence wedges.

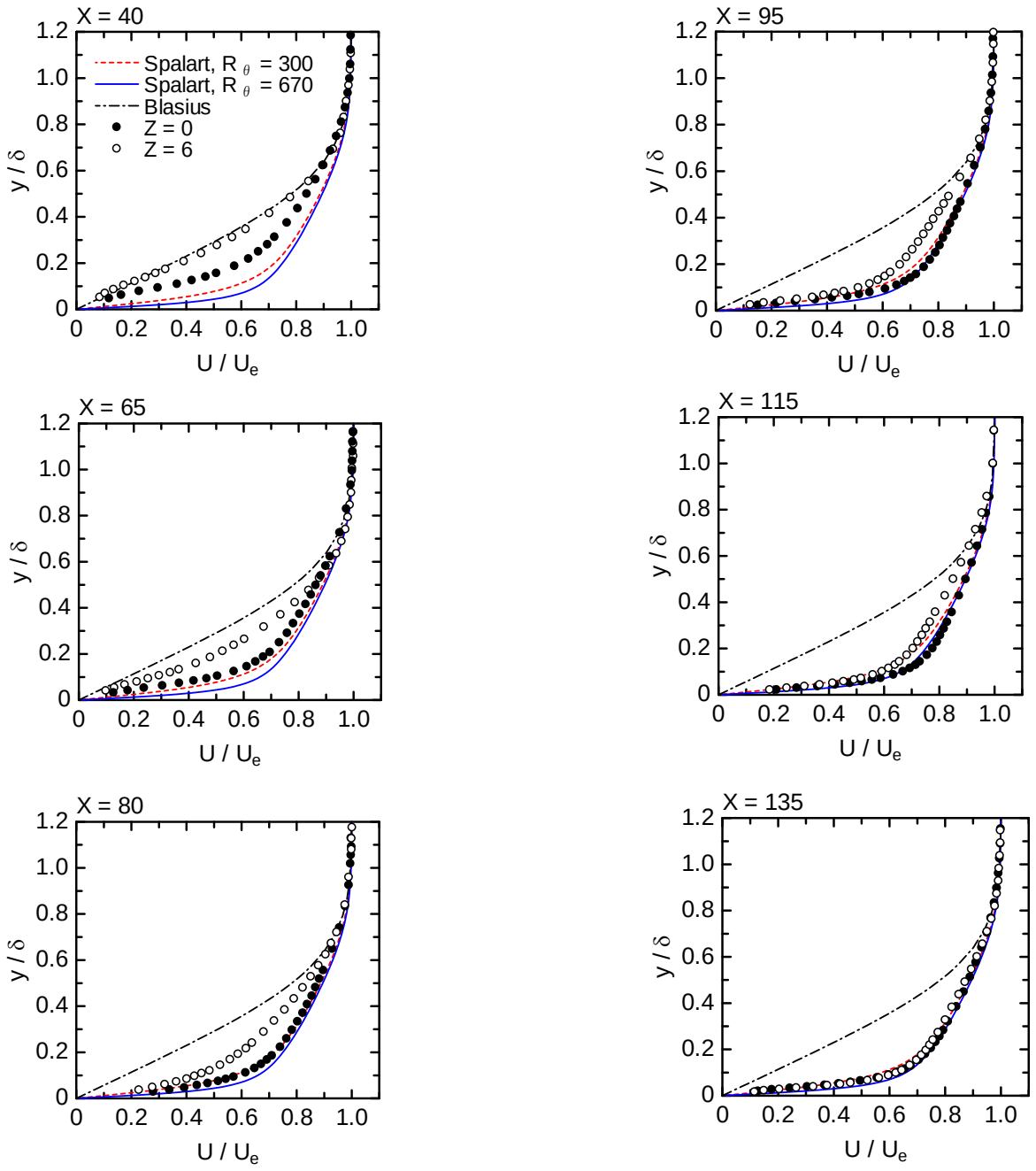

Figure 2. Mean velocity profiles.

period. The velocity distributions were so symmetric with respect to the center of each roughness element that the experimental results can be shown in a half-pitch region between roughness elements ($0 \leqq Z \leqq 6$).

Results and Discussion

Mean Velocity Distribution

Figure 2 shows mean velocity profiles on the center line of the roughness element, $Z = 0$ and on the mid-point of the roughness elements, $Z = 6$. Here, the mean velocity and the normal distance are normalized by the velocity at the edge of the boundary layer, U_e and boundary layer thickness, δ, respectively. DNS results in two Reynolds number of Spalart [6] on the turbulent boundary layer and Blasius distribution of laminar boundary layer are indicated in Fig. 2. Here, R_θ is 195 at $X = 40$, $Z = 0$, R_θ is 410 at $X = 135$, $Z = 0$ and R_θ is 480 at $X = 135$, $Z = 6$.

At first, the distributions at $Z = 0$ are examined. At $X = 40$, they do not coincide with Spalart distribution or Blasius distribution. Therefore, they do not sufficiently develop into turbulent flow, whereas further downstream, they do. At $X = 95$, it coincides with Spalart distribution. From there, the distribution form does not change downstream.

Next, the distributions at $Z = 6$ are examined. At $X = 40$, they coincide with Blasius distribution due to the fact that this station is outside of the turbulence wedge. Further downstream, as this spanwise station enters the turbulence wedge, the profile almost coincides with Spalart distribution at $X = 135$. Downstream of this station, the profile does not change, and both the profiles of $Z = 0$ and $Z = 6$ coincide. The two-dimensional boundary layer can be regarded as established there.

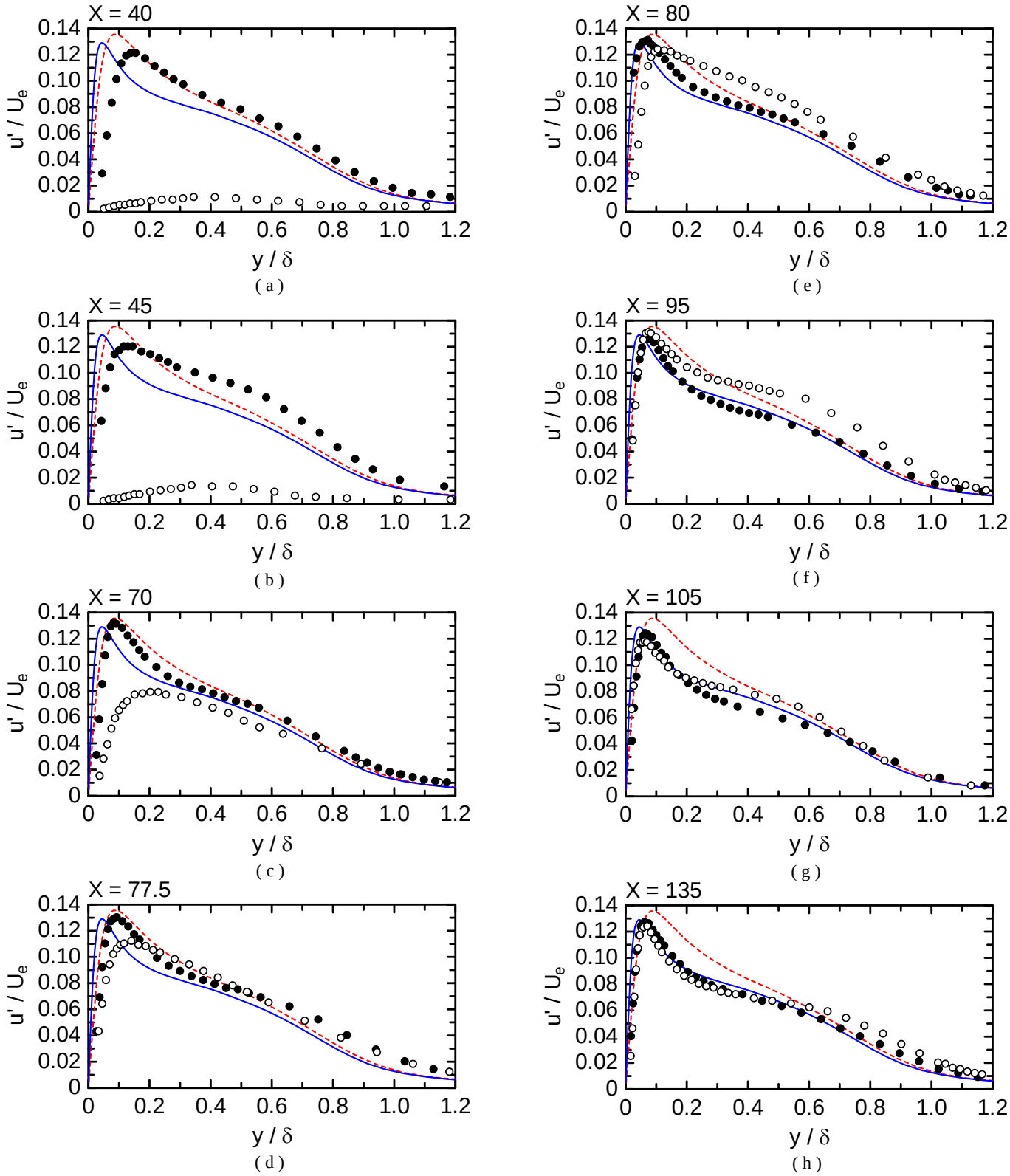

Figure 3. Wall-normal distribution of streamwise fluctuating velocities.

Fluctuating Velocity Distribution

Figure 3 shows wall-normal distribution of streamwise fluctuating velocities at Z = 0 and 6. DNS results of Spalart [6] on turbulent boundary layer in two Reynolds numbers R_θ = 300 and R_θ = 670(S300 and S670) are incorporated into the figures. They are shown in eight representative streamwise stations; before the interference of two turbulence wedges, X = 40 and 45; around the interference position, X = 70, 77.5 and 80; and after the interference, X = 95, 105 and 135.

First, we examine the distribution on the center line of the roughness element, Z = 0. At X = 40, the distribution coincides with S300 except for near the wall. At X = 45, it overshoots S300 except for near the wall. The overshoot is maximum at this station. Downstream, it decreases and undershoots S300, and finally coincides with S670 at X = 95. From there, the distribution

form does not change downstream. The boundary layer may be regarded as fully-developed turbulence. In addition to a maximum value around $y / \delta = 0.1$, "relaxation" of decrease can be seen in a region of $0.4 \leqq y / \delta \leqq 0.8$. The maxima and relaxation appear simultaneously.

Next, the distribution at the mid-point of roughness elements, $Z = 6$ are examined. At $X = 40$ and 45, the values are small, as these stations are outside of the turbulence wedges. At $X = 70$, the fluctuating velocity increases due to the interference of the two wedges.

Figure 4 compares fluctuating velocity in two conditions; one is a line of roughness elements, and the other is a single roughness element. The streamwise station, $X = 75$, is just after the interference of two wedges. The fluctuating velocity of the line of roughness elements is larger than that of a single roughness element near the wall because of the interference of the two adjacent wedges.

At $X = 77.5$, Figure 3(d), the distribution coincides with S300 except for near the wall. At $X = 80$, it overshoots S300 except for near the wall. The overshoot is maximum at this station. Figure 5 shows streamwise fluctuating velocity at the respective maximum-overshoot value stations. Maximum-overshoot values of both stations are almost the same. Then, the distribution

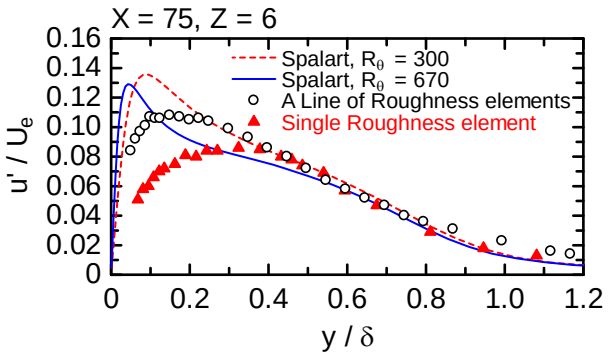

Figure 4. Comparison between a line of roughness elements and single roughness element.

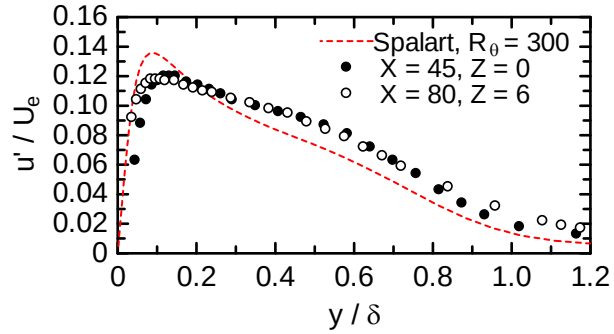

Figure 5. Fluctuating velocity at respective maximum overshoot value station.

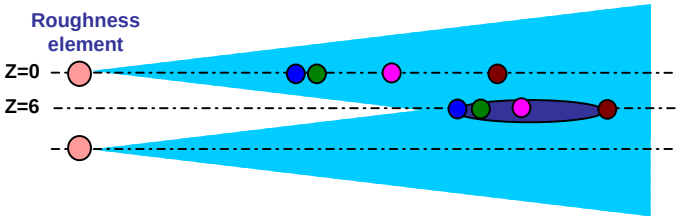

Figure 6. Schematic diagram of overshoot and undershoot process of S300 at $Z = 0$ and $Z = 6$.

decreases and undershoots S300 at $X = 105$ (Figure 3(g)). Finally, it coincides with S670 at $X = 135$. From there, the distribution form does not change downstream. The boundary layer may be regarded as fully-developed. In addition to a maximum value around $y / \delta = 0.1$, the "relaxation" of decrease can be seen in a region of $0.4 \leqq y / \delta \leqq 0.8$. The maximum value around $y / \delta = 0.1$ can be seen at $X = 70$. At $X = 95$, the relaxation ($0.4 \leqq y / \delta \leqq 0.8$) can be seen. Therefore, the manner of velocity fluctuation differs between $Z = 0$ and $Z = 6$.

Figure 6 shows a schematic diagram of typical stations of above-mentioned transition in the process of velocity fluctuation. Blue circles indicate the stations where the distribution coincides with S300 at first. Green circles show stations where the distribution most overshoots S300. Red circles indicate stations where the distribution almost coincides with S300. And brown circles mean stations where the distribution finally coincides with S670. These processes are seen with both $Z = 0$ and $Z = 6$. The process appears from more upstream at $Z = 0$ than $Z = 6$. The transition process is induced by the roughness element at $Z = 0$, whereas it is induced by the interference of two adjacent wedges at $Z = 6$. Downstream of $X = 135$, the distribution does not change. Both distribution of $Z = 0$ and $Z = 6$ coincide. The two-dimensional boundary layer can be regarded as established there.

Conclusions

Experiments were performed to investigate the effect of a line of three-dimensional roughness elements on boundary-layer transition on a flat-plate with zero pressure gradient. The following conclusions were obtained.

(1) At first, the fluctuating velocity overshot Spalart distribution of DNS ($R_\theta = 300$). Next, it decreased and undershot the distribution, and finally coincided with it ($R_\theta = 670$). These processes appeared more upstream at $Z = 0$ than $Z = 6$.

(2) The transition process is induced by the roughness element at $Z = 0$, whereas it is induced by the interference of the two adjacent wedges at $Z = 6$.

(3) Maximum-overshoot values of both spanwise positions are almost the same.

(4) Downstream of $X = 135$, the distribution does not change. Both distribution of $Z = 0$ and $Z = 6$ coincide. The two-dimensional boundary layer can be regarded as established there.

References

[1] Gibbings, J.C., Goksel, O.T. & Hall. D.J., The Influence of Roughness Trips upon Boundary-Layer Transition, Part 3. Characteristics of Rows of Spherical Transition Trips, *Aeron. J.*, **90**-900, 1986, 393-398.

[2] Gregory, M.A. & Walker, W.S., The Effect on Transition of Isolated Surface Excrescences in the Boundary Layer, *ARC R. & M.*, 2779, 1951.

[3] Ichimiya, M., Nakase, Y. and Fukutomi, J., Structure of a Turbulence Wedge Developed from a Single Roughness Element on a Flat Plate, in *Engineering Turbulence Modelling and Experiments 2*, editors W. Rodi and F. Martelli, Elsevier, 1993, 613-622.

[4] Ichimiya, M., The Effect of a Single Roughness Element on a Flat Plate Boundary Layer Transition, in *Engineering Turbulence Modelling and Experiments 4*, editors W. Rodi and D. Laurence, Elsevier, 1999, 597-606.

[5] Mochizuki, M., Smoke Observation on Boundary Layer Transition Caused by a Spherical Roughness Element, *J. Phys. Soc. Jpn.*, **16**-5, 1961, 995-1008.

[6] Spalart, P.R., Direct Simulation of a Turbulent Boundary Layer up to $R_\theta = 1410$, *J. Fluid Mech.* **187**, 1988, 61-98.

[7] Tani, I., Komoda, H., Komatsu, Y. & Iuchi, M., Boundary-Layer Transition by Isolated Roughness, *Aeron. Res. Inst. Univ. Tokyo Rep.*, **375**, 1962, 129-143